LIM-domain protein cysteine- and glycine-rich protein 2 (CRP2) is a novel marker of hepatic stellate cells and binding partner of the protein inhibitor of activated STAT1

Ralf WEISKIRCHEN*[1], Markus MOSER†, Sabine WEISKIRCHEN*, Martin ERDEL‡, Sandra DAHMEN†, Reinhard BUETTNER§ and Axel M. GRESSNER*

*Institute of Clinical Chemistry and Pathobiochemistry, RWTH-University Hospital, Pauwelsstrasse 30, D-52074 Aachen, Germany, †Institute of Pathology, RWTH-University Hospital, Pauwelsstrasse 30, D-52074 Aachen, Germany, ‡Institute of Medical Biology and Human Genetics, University of Innsbruck, A-6020 Innsbruck, Austria, and §Institute of Pathology, University Hospital Bonn, D-53127 Bonn, Germany

Activation of hepatic stellate cells is considered to be the main step in the development of liver fibrosis, which is characterized by the transition of quiescent vitamin-A-rich cells to proliferative, fibrogenic and contractile myofibroblasts. The identification of regulatory genes during early cell activation and transdifferentiation is essential to extend our knowledge of hepatic fibrogenesis. In liver, the gene *CSRP2* is exclusively expressed by stellate cells, whereas no transcripts are detectable in hepatocytes, sinusoidal endothelial cells or Kupffer cells. The early activation of stellate cells induced by platelet-derived growth factor is accompanied by an enhanced expression of *CSRP2*. During later stages of transdifferentiation, the expression of *CSRP2* in these cells is suppressed *in vitro* and *in vivo*. The *CSRP2*-encoded cysteine- and glycine-rich double-LIM-domain protein (CRP)2 is proposed to function as a molecular adapter, arranging two or more as yet unidentified protein constituents into a macromolecular complex. To identify these proteins and assign a cellular function to CRP2, a human cDNA library was screened with full-length CRP2 as bait in a yeast two-hybrid screen. The protein inhibitor of activated STAT1 ('PIAS1') was shown to associate selectively with the C-terminal LIM domain of CRP2. Physical interaction of both proteins in the cellular environment was confirmed by co-localization experiments with confocal laser scanning microscopy and co-immunoprecipitation analysis. These results establish CRP2 as a potential new factor in the JAK/STAT-signalling pathway and suggest that the suppression of *CSRP2* might be a prerequisite for the myofibroblastic transition of hepatic stellate cells.

Key words: bile duct ligation, JAK/STAT pathway, LIM-domain proteins, liver fibrosis, platelet-derived growth factor.

INTRODUCTION

Members of the cysteine- and glycine-rich protein (CRP) family are characterized by the presence of two tandemly arranged LIM domains linked to short glycine-rich regions [1]. So far, three members of the CRP family (CRP1, CRP2 and CRP3/MLP, in which MLP stands for muscle LIM-domain protein) have been characterized in vertebrates [2–4]. They exhibit a tissue-specific distribution with a unique dual subcellular localization [5,6]. CRP1 expression is detected in a variety of organs enriched in smooth muscle, CRP2 is restricted to arteries and fibroblasts, and CRP3/MLP is dominant in organs enriched in striate muscle [3,7,8]. Mice deficient in CRP3/MLP exhibit defects in the architecture and function of both striate and cardiac muscle [9]. Biochemical studies as well as immunofluorescence experiments suggest that CRPs are involved in promoting protein assembly along the actin-based cytoskeleton [7,10]. As a common biochemical property they can associate with the actin cytoskeleton and are capable of interacting with α-actinin and zyxin when overexpressed in adherent fibroblasts [5,7,11]. The C-terminal LIM domain (LIM2) of each CRP is predicted to have at least one protein partner and it was recently demonstrated that CRP3/MLP, but not CRP1 or CRP2, interacts in the cytosolic compartment with βI-spectrin [12]. CRP3/MLP also interacts with the basic helix–loop–helix myogenic transcription factors MyoD, myogenin and MRF4, increasing their affinity for specific DNA regulatory elements [6]. *CSRP2*, encoding the CRP2 protein, was originally isolated on the basis of its strong transcriptional suppression in fibroblasts transformed by viral oncogenes or chemical carcinogens [3]. Conditional cell transformation reveals that CRP2 is essential to the maintenance of normal cell function [1,13]. The expression is strongly decreased in vascular smooth-muscle cells in response to platelet-derived growth factor (PDGF) or vessel wall injury induced by balloon injury of the carotid artery [14]. Common to the process of cell transformation and wound healing is a modified cytokine response of injured cells. Whereas PDGF is expressed at low levels in arteries from healthy adults, its expression is increased in conjunction with the inflammatory–fibroproliferative response that characterizes atherosclerosis [15]. It is noteworthy that both the injury of arterial tissue by balloon catheter and experimentally induced atherosclerosis are associated with an increased ex-

Abbreviations used: α-SMA, α-smooth-muscle actin; CRP, cysteine- and glycine-rich protein; DAPI, 4,6-diamidino-2-phenylindole; DMEM, Dulbecco's modified Eagle's medium; FCS, fetal calf serum; FISH, fluorescence *in situ* hybridization; GAPDH, glyceraldehyde-3-phosphate dehydrogenase; HBSS, Hanks buffered standard saline; HSCs, hepatic stellate cells; LIM1, N-terminal LIM domain of CRP; LIM2, C-terminal LIM domain of CRP protein; MFBs, myofibroblastic cells; MLP, muscle LIM-domain protein, PDGF, platelet-derived growth factor; PIAS1, protein inhibitor of activated STAT1, TGF-β_1, transforming growth factor β_1; X-Gal, 5-bromo-4-chloroindol-3-yl β-D-galactopyranoside.

[1] To whom correspondence should be addressed (e-mail rweiskirchen@post.klinikum.rwth-aachen.de).

© 2001 Biochemical Society

pression of PDGF and up-regulation of PDGF receptors. This polypeptide growth factor is also thought to have a pivotal role in the cascade of events resulting in liver fibrosis, which is the wound-healing response to a variety of chronic inflammatory insults such as primary biliary cirrhosis, chronic hepatitis and toxic damage by alcohol. In necroinflammatory injury, quiescent hepatic stellate cells (HSCs) transdifferentiate to proliferatively active myofibroblastic cells (MFBs). Increasing numbers of HSCs during liver fibrogenesis arise from local proliferation in response to polypeptide growth factors [16,17]. This fibrogenic activation is associated with the synthesis of PDGF and its receptors [18]. The aim of this study was to investigate the expression of *CSRP2* in liver and to evaluate possible changes in its expression in injured liver and activated HSCs. Cell activation was induced either *in vitro* by culturing quiescent HSCs on a plastic surface or in an *in vivo* model of hepatic fibrosis induced by ligation of the common bile duct. We show that *CSRP2* in liver is restricted to HSCs and that its expression is tightly controlled during the activation process. On the basis of the notion that CRP2 is a molecular adapter protein [19], we also performed a yeast two-hybrid screen to identify possible binding partners of CRP2. We found that CRP2 associates via its LIM2 domain with the protein inhibitor of activated STAT1 (PIAS1), which is a strong suppressor of the JAK/STAT (Janus kinase/signal transduction and activators of transcription) pathway [20]. On the basis of our results we propose that CRP2 might modulate a variety of developmentally and pathophysiologically relevant processes by interacting with essential mediators of cytokine-regulated pathways.

EXPERIMENTAL

Isolation and culture of rat liver cells

Male Sprague–Dawley rats had access to Altromin chow and water *ad libitum*. Hepatocytes were isolated by the collagenase method of Seglen [21], with slight modifications. In brief, animals were anaesthetized and liver was preperfused *in situ* via the portal vein followed by recirculating perfusion *ex situ*. Thereafter, the liver was perfused with collagenase and the capsule was gently removed. The tissue was dissected under constant swirling and the cell suspension obtained was subsequently filtered through nylon mesh (250 and 100 μm pore sizes), centrifuged and washed three times. Cells were seeded in DMEM (Dulbecco's modified Eagle's medium) (Bio Whittaker Europe, Verviers, Belgium) supplemented with 10 % (v/v) FCS (fetal calf serum; Seromed, Berlin, Germany), 4 mM L-glutamine (ICN Biomedicals, Aurora, OH, U.S.A.), 100 i.u./ml penicillin, 100 μg/ml streptomycin and 0.02 i.u./ml bovine pancreas insulin. HSCs, Kupffer cells and sinusoidal endothelial cells were isolated by the pronase–collagenase method [22]. Livers were therefore subsequently perfused with HBSS (Hanks buffered standard saline) (PAA Laboratories GmbH, Linz, Austria), with 0.35 % (w/v) pronase E in HBSS and with 0.015 % (w/v) collagenase in HBSS. Thereafter, livers were homogenized under permanent pH control (pH 7.3) in HBSS containing 100 μg/ml DNase type II (Roche, Mannheim, Germany). The suspension was filtered through nylon mesh, centrifuged and washed in ice-cold HBSS containing 0.25 % BSA. HSCs were further purified by single-step density gradient centrifugation with 8.25 % (w/v) Nycodenz® (Nycomed Pharma AS, Oslo, Norway) as described in detail elsewhere [23]. Kupffer cells and sinusoidal endothelial cells were collected by centrifugal elutriation [24,25] in a JE-5.0-type rotor equipped with a standard separation chamber in a Beckman model Avanti™ J-20 centrifuge. HSCs were seeded in DMEM, Kupffer cells in RPMI medium (Biochrom KG, Berlin, Germany), both supplemented with FCS, L-glutamine, penicillin and streptomycin. RNA from sinusoidal endothelial cells was directly extracted without prior cell cultivation. The purity of cell preparations was assessed by light microscopic appearance and positive immunofluorescence stainings [26]. For cytokine stimulation, HSCs were treated 2 days after seeding with 40 ng/ml recombinant rat PDGF-BB (R&D Systems, Wiesbaden, Germany) or 10 ng/ml recombinant transforming growth factor β_1 (TGF-β_1; R&D Systems) for 48 h.

RNA isolation and Northern analysis

Isolation and Northern analysis of RNA from rat liver cells or human cell line WI-26 VA4 (A.T.C.C., Manassas, VA, U.S.A.) were performed as described previously [3]. RNA from human kidney biopsies and rat livers was extracted after homogenization with an Ultra-Turrax® (type TP18/10) and shearing DNA by pressing the resulting lysate three times through a 20-gauge needle before RNA isolation. Purified RNA was resuspended in water and the concentration was determined by UV absorbance.

Experimental model of cholestatic liver fibrosis

Male Sprague–Dawley rats (200–250 g body weight) were subjected to double ligature of the common bile duct with intersectional scission under anaesthesia [27]. Sham-operated rats that underwent laparotomy without bile duct ligation served as controls. The animals were killed 20 days after surgery. Before death, blood was aspirated from the portal vein and sera were analysed for alanine aminotransferase, aspartate aminotransferase and bilirubin to prove cholestasis and liver damage. Tissue pieces for *in situ* hybridization were directly fixed in 4 % (w/v) paraformaldehyde and embedded in paraffin. Cryostat sections for immunohistochemistry or staining with Oil Red O were snap-frozen in solid CO_2.

Immunohistochemistry and staining with Oil Red O

A monoclonal antibody directed against α-smooth-muscle actin (α-SMA) (clone 1A4; Dako, Hamburg, Germany) was used to detect the expression of α-SMA. Immunohistochemical stainings were performed with indirect immunoperoxidase. In brief, paraffin-embedded 4 μm tissue sections were incubated with the α-SMA-specific antibody (1:500 dilution); a biotin-linked anti-mouse IgG (1:500 dilution) was used as the secondary antibody. Immunoreactions were detected with the Vectastain-ABC kit (Vector Laboratories, Burlingame, CA, U.S.A.). Sections were counterstained with haematoxylin or haematoxylin–eosin. For Oil Red staining, rat liver cryostat sections were stained with 0.3 % (w/v) Oil Red O (Sigma, Deisenhofen, Germany) in 60 % (v/v) propan-2-ol for 10 min, washed in water and counterstained with haematoxylin or haematoxylin–eosin.

In situ hybridization of CSRP2 mRNA in mouse embryos and rat liver sections

The *Eco*RI fragment of pCRIII-rSmLIM [14] was cloned into pSPT18 (Roche). To generate riboprobes the plasmid was linearized with *Pvu*II or *Pst*I and sense and anti-sense transcripts were produced with either the SP6 or the T7 RNA polymerase. Paraffin-embedded sections of NIH Swiss mouse embryos were pretreated with proteinase K (10 μg/ml) for 30 min at 37 °C, fixed in 4 % (v/v) paraformaldehyde/PBS (pH 7.0) for 5 min, washed twice in water and acetylated in acetic anhydride diluted 1:400 in 0.1 M triethanolamine (pH 8.0) for 10 min at room temperature. Slides were then washed twice in water, dehydrated

© 2001 Biochemical Society

in ethanol, dried in air and prehybridized for 4 h at 50 °C in hybridization solution containing 50 % formamide, 10 % dextran sulphate, 10 mM Tris/HCl, pH 8.0, 10 mM sodium phosphate buffer, pH 7.0, 2 × SSC (where SSC is 0.15 M NaCl/0.015 M sodium citrate), 5 mM EDTA (final pH of solution, pH 8.0), 150 μg/ml tRNA, 10 mM dithiothreitol and 10 mM 2-mercaptoethanol. Hybridizations were performed overnight in the same mix supplemented with 5×10^4 c.p.m./μl sense or anti-sense riboprobes at 50 °C. The slides were washed twice at 52 °C in 50 % formamide/2 × SSC for 30 min. After treatment with RNase A (20 μg/ml) for 30 min at 37 °C, slides were washed five times with 50 % formamide/2 × SSC at 55 °C for 1 h, rinsed in 2 × SSC, dehydrated, coated with Kodak NTB2 emulsion and exposed to X-ray film for appropriate durations.

Construction of yeast expression plasmids

DNA corresponding to full-length human CRP2, amino acid residues 1–82 (LIM1) or residues 83–193 (LIM2) of human CRP2 was amplified by PCR with human *CSRP2* cDNA as template [28]. The following primers were used: 5′-d(GAATTCATGCCTGTCTGGGGAGGTGG)-3′ (P1) and 5′-d(CCATGGTTACTGGGCATGAACAAGAG)-3′ (P2) for full length CRP2; P1 and 5′-d(CCTAGTTAAGCGTGCCAGCGCC)-3′ (P3) for LIM1; and 5′-d(GAATTCATGGACCGTGGCGAGAGG)-3′ (P4) and P2 for LIM2. Cycling products were ligated into the pGEM-T-Easy vector (Promega, Madison, WI, U.S.A.) and the integrity of cloned fragments was confirmed by sequencing. Restriction sites (underlined) introduced by PCR (*Eco*RI, *Nco*I) or included in the multiple cloning site of pGEM-T-Easy (*Eco*RI) were used to subclone into expression plasmid pLexA [29], generating plasmids pLexA(hCRP2), pLexA [hCRP2(LIM1)] and pLexA[hCRP2(LIM2)], respectively. For the construction of pLexA(qCRP2) encoding full-length quail CRP2, the *Not*I fragment from clone W15 [3] was filled in by Klenow DNA polymerase and cloned into the filled-in *Bam*HI site of pLexA.

Yeast two-hybrid interaction assays

Yeast cultures were grown under standard conditions in liquid medium or on solid medium with minimal synthetic dropout medium (Clontech, Heidelberg, Germany). All yeast transformations were performed by using a standard TE/lithium acetate method [30] with established modifications [31–33]. In brief, the reporter strain EGY48/p8op-*lacZ* [34,35] was sequentially transformed with bait plasmid pLexA(hCRP2) and a human kidney Matchmaker LexA prey cDNA library (Clontech) cloned into pB42AD [29]. Transformants were screened for leucine auxotrophic marker (Leu) and β-galactosidase (β-gal) activity. For characterization of individual positives, total yeast DNA preparation was performed with a glass beads/phenol/chloroform embedded method [36]. With this DNA as template and with primers 5′-d(CCAGCCTCTTGCTGAGTGGAGATG)-3′ (P5) and 5′-d(GCAACCTGACCTACAGGAAAGAG)-3′ (P6), selective amplification of prey inserts by PCR was performed. PCR products were directly sequenced with primer P5. For the selective rescue of interesting prey vectors, total yeast DNA was transformed into *Escherichia coli* KC8 cells (*hsdR*, *leuB600*, *trpC9830*, *pyrF*::*Tn5*, *hisB463*, *lac*Δ*X74*, *strA*, *galU*, *galK*) and selected on M9 plates supplemented with ampicillin and thiamine. To determine the binding site of CRP2 with PIAS1, EGY48/p8op-*lacZ* yeast cells were simultaneously transformed with prey clone pB42AD-no75 and individual bait constructs. Selected transformants were picked and tested for reporter activity on minimal plates lacking Leu and supplemented with 40 μg/ml 5-bromo-4-chloroindol-3-yl β-D-galactopyrano side (X-Gal).

Construction of mammalian expression vectors

The 1305 bp *Eco*RI and *Xho*I fragment of pB42AD-no75 was filled in by Klenow DNA polymerase and ligated into pCMV-Myc (Clontech), which had been cut by *Sal*I and filled in. To construct pCMV-Myc-hCRP2 and pCMV-HA-hCRP2 the 592 bp blunted *Eco*RI/*Nco*I fragment of pLexA-hCRP2 was ligated into the filled-in *Sal*I site of pCMV-Myc or pCMV-HA (Clontech) respectively.

Indirect immunofluorescence and confocal laser-scanning microscopy

NIH-3T3 cells were grown in DMEM supplemented with 10 % FCS, 4 mM L-glutamine, 100 i.u./ml penicillin and 100 μg/ml streptomycin. Coverslips for indirect immunofluorescence were preincubated in medium, rinsed in PBS and placed in six-well dishes. Approximately 3×10^5 cells in 2 ml were added to each dish and, after incubation for 16 h at 37 °C, cells were transfected using the FuGENE™6 method (Roche). After incubation for 30 h, coverslips were washed three times in ice-cold PBS and cells were fixed for 15 min in 4 % (w/v) paraformaldehyde buffered in PBS (pH 7.4). Cells were then permeabilized for 2 min on ice in a solution containing 0.1 % sodium citrate and 0.1 % (v/v) Triton X-100 followed by three washes in PBS. Thereafter, cells were blocked for 30 min at 37 °C in 50 % (v/v) FCS/0.1 % BSA in PBS and in 1 % (w/v) BSA/0.1 % fish gelatin in PBS. After washing, incubations with appropriate antibody solutions were performed at 37 °C for 1 h each in 0.1 % BSA in PBS followed by three washes in PBS. To reveal protein distributions, samples were analysed by confocal laser scanning microscopy (LS 410 Invert; Zeiss, Oberkochen, Germany). Fluorescent dye labels were monitored simultaneously with a standard objective (40 × 1.3 oil immersion), an external Ar laser (488 nm excitation, FITC signals) and an internal He/Ne laser (543 nm excitation, Cy-3 signals). Documentation was performed in either overlay mode or frame mode (consecutive overlay). Samples were analysed in confocal mode without sectioning, with an internal zoom factor of 3.0. A CRP2-specific antiserum [37], a monoclonal anti-Myc antibody (clone 9E10; Clontech), a pre-adsorbed goat anti-(mouse-IgG) Cy-3 (Dianova, Hamburg, Germany), a biotinylated pig anti-(rabbit IgG) (Dako), a streptavidin–FITC conjugate (Dako) and a murine control IgG1 fraction (Santa Cruz, CA, U.S.A.) were used.

Co-immunoprecipitation

Transiently expressed Myc-CRP2 (or HA-CRP2) and Myc-PIAS1 were co-immunoprecipitated from the HEK-293 cell line with a polyclonal CRP2 antibody [37]. Immunopreciptation was performed using a protocol described previously [38]. Cell lysates for precipitation were prepared by lysing approx. 2×10^7 cells in 0.5 ml of immune precipitation assay buffer containing 1 % (v/v) Nonidet P40, 0.25 % sodium deoxycholate, 150 mM NaCl and 50 mM Tris/HCl, pH 7.5, supplemented with proteinase inhibitors (Roche). Immunocomplexes were recovered by the addition of 50 μl Protein A–Sepharose beads (Santa Cruz) and separated by SDS/PAGE. After transfer on to nitrocellulose membranes (0.45 μm pore size; Schleicher & Schuell) the blots were probed with a monoclonal antibody against the Myc epitope followed by incubation with an anti-mouse IgG coupled to horseradish peroxidase. Horseradish peroxidase signals were detected with the Super signal detection system (Pierce).

© 2001 Biochemical Society

Chomosomal mapping by fluorescence *in situ* hybridization (FISH)

FISH and chromosomal assignment were performed as described previously [28]. In brief, metaphase spreads were prepared from phytohaemagglutinin-stimulated human peripheral blood lymphocytes. The PIAS1 cDNA was labelled with biotin-16-dUTP in nick translation and was directly hybridized to the metaphase spreads. For the detection of hybridized biotinylated DNA, goat anti-biotin and rabbit anti-goat antibodies conjugated to FITC were used. Chromosomes and the exact subchromosome signal locations were identified by 4,6-diamidino-2-phenylindole (DAPI) banding and by linear interpolation of fluorescent peaks to standard chromosome ideograms with quantitative image-analysing software.

Sequence analysis

All primers were obtained from MWG-Biotech AG (Ebersberg, Germany) and sequencing was done with the ABI Prism BigDye® termination reaction kit (PE Applied Biosystems, Weiterstadt, Germany). Each cycle sequencing reaction contained 8 μl of BigDye® termination reaction mix, 30 ng of primer and 1 μg of plasmid (or 200 ng of PCR fragment). The cycling conditions were as follows: initial denaturation at 95 °C for 5 min, followed by 50 cycles at 95 °C for 30 s, 55 °C for 20 s and 60 °C for 4 min. Products were purified on Centri-Sep spun columns (Princeton Separations, Adelphia, NJ, U.S.A.), dried in a Speed Vac system, resuspended in 20 μl of template suppression reagent, denatured at 95 °C for 2 min and then separated on the ABI Prism 310 Genetic Analyzer (PE Applied Biosystems) automatic sequencer.

RESULTS

Expression of *CSRP2* in rat liver

To establish *CSRP2* expression in rat liver a Northern-blot analysis was performed with RNA extracted from the component cells of hepatic origin and kidney as a control (Figure 1A). A single transcript 1.0 kb in size was visible exclusively in HSCs and to a smaller extent in their transdifferentiated phenotype, i.e. the MFB. *CSRP2* transcripts were virtually absent from whole liver, hepatocytes, sinusoidal endothelial cells and Kupffer cells. Thus, in liver, *CSRP2* reveals a highly restricted cellular expression pattern. Subsequent analysis revealed that *in vitro* the activation of HSCs is accompanied by an initial moderate up-regulation of *CSRP2* expression with a peak at the seventh day of primary culture. At later stages of transdifferentiation there was almost complete loss of *CSRP2* transcripts in such cells (Figure 1B). In these analyses, the level of mRNA encoding the enzyme glyceraldehyde-3-phosphate dehydrogenase (GAPDH) was used as an internal standard for the quality and amount of RNA present in each lane.

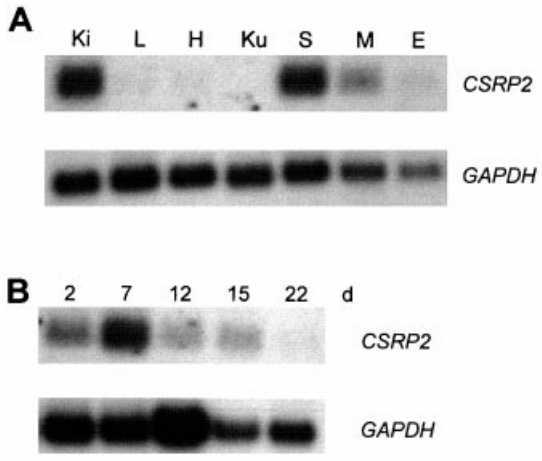

Figure 1 Expression of *CSRP2* in isolated liver cells

(**A**) 10 μg portions of total RNA from kidney (Ki), whole liver (L), hepatocytes (H), Kupffer cells (Ku), HSCs (S), myofibroblasts (M) and hepatic sinusoidal endothelial cells (E) were separated on a 1.3% (w/v) denaturing agarose gel, transferred on to a nylon membrane and hybridized with a [α-^{32}P]dCTP-labelled rat-specific *CSRP2* cDNA probe. (**B**) RNA from HSCs/MFBs on the 2nd, 7th, 12th, 15th and 22nd days in primary (2 and 7 days), secondary (12 and 15 days) or tertiary (22 days) culture was hybridized with a *CSRP2*-specific probe. Filters (**A**, **B**) were rehybridized with a GAPDH-specific probe to verify equivalent loading.

To rule out the possibility that the observed exclusive expression of *CSRP2* in HSCs occurs only in cultured cells we performed *in situ* hybridization. The specificity of the *CSRP2* anti-sense riboprobe was first demonstrated by *in situ* hybridizations with paraffin-embedded murine embryo specimens (Figure 2A). The specific hybridization signals visible in the cardiovascular system, kidney, cortex and defined regions of the gastrointestinal tract were in agreement with previous reports [14]. No cross-hybridization was detectable with riboprobes in the sense orientation (results not shown). In sections of normal liver, *CSRP2*-specific signals were detected in the parasinusoidal space of Disse (Figures 2B and 2C). These observations agree with our Northern-blot analysis and indicate that *CSRP2* was also expressed *in vivo* exclusively in HSCs. To analyse whether the expression was changed during fibrogenesis in the setting of cholestatic liver injury, we used the model based on ligation of the common bile duct. At 20 days after surgery, animals showed the typical ductular reactions and ongoing liver fibrogenesis. In comparison with normal liver, drastic changes in architecture were observed by visual inspection of haematoxylin-stained sections (Figures 3A and 3B) and immunostaining for α-SMA (Figures 3C and 3D). In control livers, cells positive for α-SMA were noted in smooth-muscle cells of portal tract vessels and in a few cells surrounding terminal hepatic venules (Figure 3C). In bile-duct-ligated rats, livers were highly enriched in α-SMA-positive HSCs forming layers around the bile ductules. In addition, α-SMA-positive cells in the periportal sinusoids were visible in the vicinity of ductular areas, which was consistent with the active recruitment of activated HSCs by ductular structures (Figure 3D). In addition, the loss of vitamin A droplets during hepatic fibrosis, as demonstrated by staining with Oil Red O, was taken as a consistent marker of successful induction of hepatic fibrosis (Figures 3E and 3F). Additionally, liver damage in these animals was further indicated by a significant elevation of serum levels for alanine aminotransferase (more than 120 units/l), aspartate aminotransferase (more than 750 units/l) and bilirubin (more than 13 mg/dl). We next examined the expression of *CSRP2* in sections of normal and fibrotic livers. In comparison with control livers, the expression of *CSRP2* along the sinusoids after bile duct ligation was markedly heterogeneous. Maximal expression was detectable in the stroma surrounding proliferating ductules (Figures 3G and 3H). Interestingly, MFBs in zones of complete fibrosis showed no expression of *CSRP2*. In summary, the results indicate (1) that the expression of *CSRP2* in liver was restricted to HSCs and (2) that the expression was influenced by cholestatic liver injury. Consistent with our results obtained *in vitro* was the observation that *CSRP2* expression was initially up-regulated during HSCs activation and was lost in MFBs.

The most effective stimulus for the proliferation of HSCs/MFBs yet described is PDGF. To investigate whether the expression of *CSRP2* during transdifferentiation is influenced by this mitogen we performed stimulation experiments (Figure 4).

© 2001 Biochemical Society

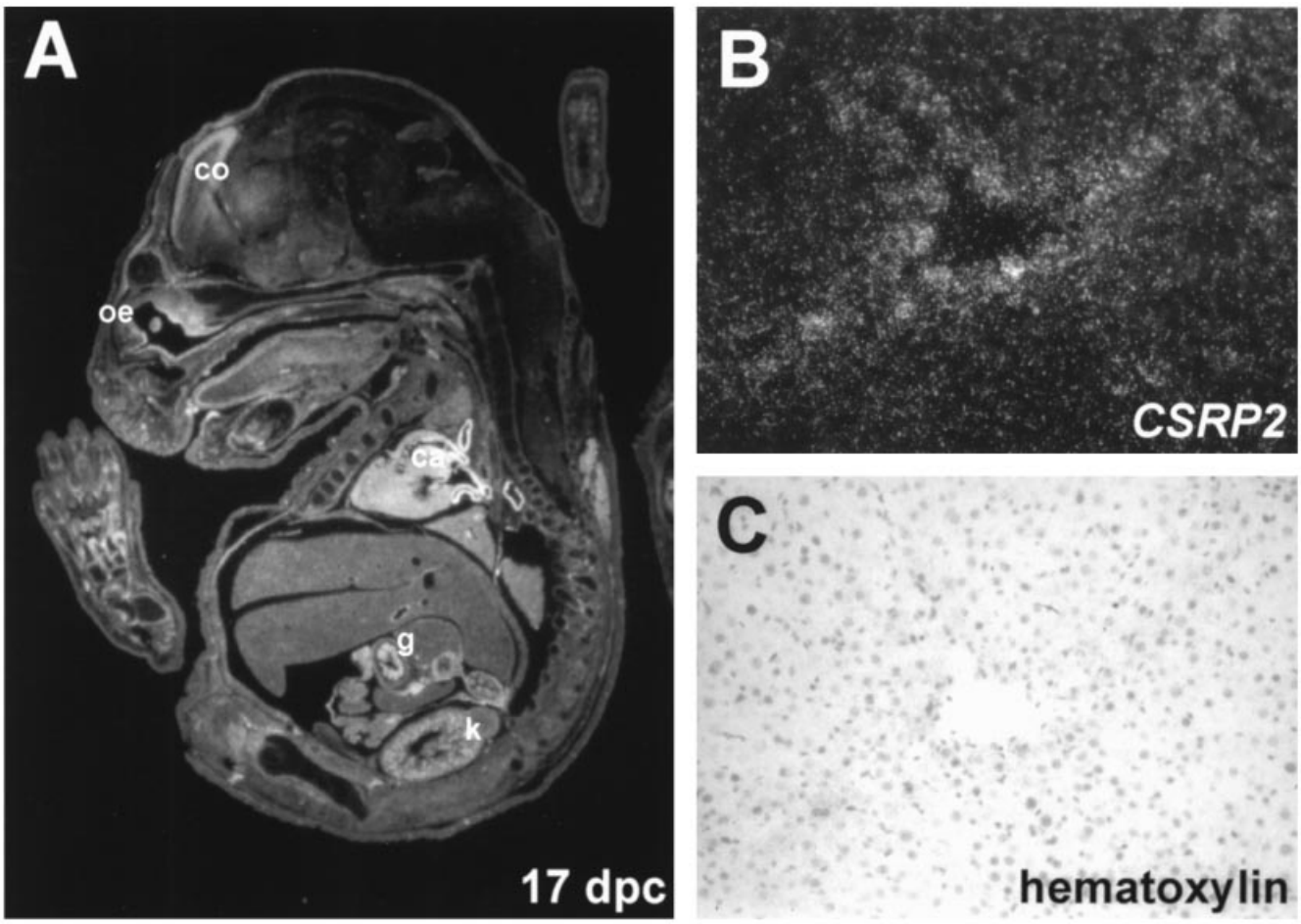

Figure 2 Expression *in vivo* of *CSRP2* analysed by *in situ* hybridization

(**A**) *In situ* hybridization analysis of murine embryo tissue sections with a *CSRP2* anti-sense probe at the 17th day of embryogenesis (magn. $\times 10$). Labelled structures are: cardiovascular system (ca), kidney (k), cortex (co), gastrointestinal tract (g), and olfactory epithelium (oe). (**B**) *In situ* hybridization analysis for *CSRP2* expression in adult rat liver (magn. $\times 100$). *CSRP2* staining is restricted to the parasinusoidal space of Disse. (**C**) Haematoxylin staining of the liver section shown in (**B**).

Administration of PDGF to HSCs resulted in an increased cell activation that was characterized mainly by retinoid loss and a phenotypic change into MFB morphology (Figures 4A and 4B). In comparison with unstimulated or TGF-β_1-treated cells, CSRP2 mRNA was significantly increased in response to PDGF (Figure 4C). Although the intensities of 28 S and 18 S rRNA species revealed that each lane was loaded with comparable amounts of RNA, the expression of GAPDH was also increased in response to PDGF. This observation is in agreement with previous reports showing significant stimulation of GAPDH expression in quiescent cells in response to PDGF [39]. Interestingly, the cell line CFSC-2G derived from a carbon-tetrachloride-cirrhotic rat liver [40] also showed no *CSRP2* expression. This cell line has a phenotype similar to transdifferentiated MFBs, as indicated by its ability to synthesize large quantities of α1(I)-procollagen, fibronectin and TGF-β, the hallmark of an MFB phenotype.

Identification of PIAS1 as a binding partner for CRP2

CSRP2 encodes the double-LIM-domain protein CRP2. This protein is proposed to function as an adapter molecule, arranging two or more protein constituents into a supramolecular complex. Although members of the CRP/MLP family have affinity for α-actinin [9], zyxin [41], basic helix–loop–helix transcription factors [6], βI-spectrin [12] and a novel protein (CRP2BP) with unknown function [37], none of the identified binding partners allows the assignment of a cellular function. In an effort to identify proteins that bind to CRP2, we used the LexA-based interaction trap [29]. This sensitive yeast-based two-hybrid system [42] was previously used to identify CRP2BP [37]. In our interacting hunt, full-length human CRP2 encoding a protein of 193 residues was chosen as the bait. Because *CSRP2* is highly expressed in human kidney (Figure 5), we decided to screen a commercially available human kidney Matchmaker library for interacting partners. In a representative screen of 4×10^8 yeast transformants with the Leu/X-Gal-based dual reporter system, we identified 89 prey clones positive for both reporters. Of these, 51 showed a Gal/Raf-dependent activation of both reporters. The clones were grouped into four major classes on the basis of their sequences (Table 1). Isolated mitochondrial proteins known to interfere non-specifically with the interaction trap (http://www.fccc.edu/research/labs/golemis/InteractionTrapInWork.html) are listed in group 1. Some identified cDNA species of cytosolic proteins (group 2) such as cyclophilin, GAPDH and uromodulin were not fused in frame to the B42

© 2001 Biochemical Society

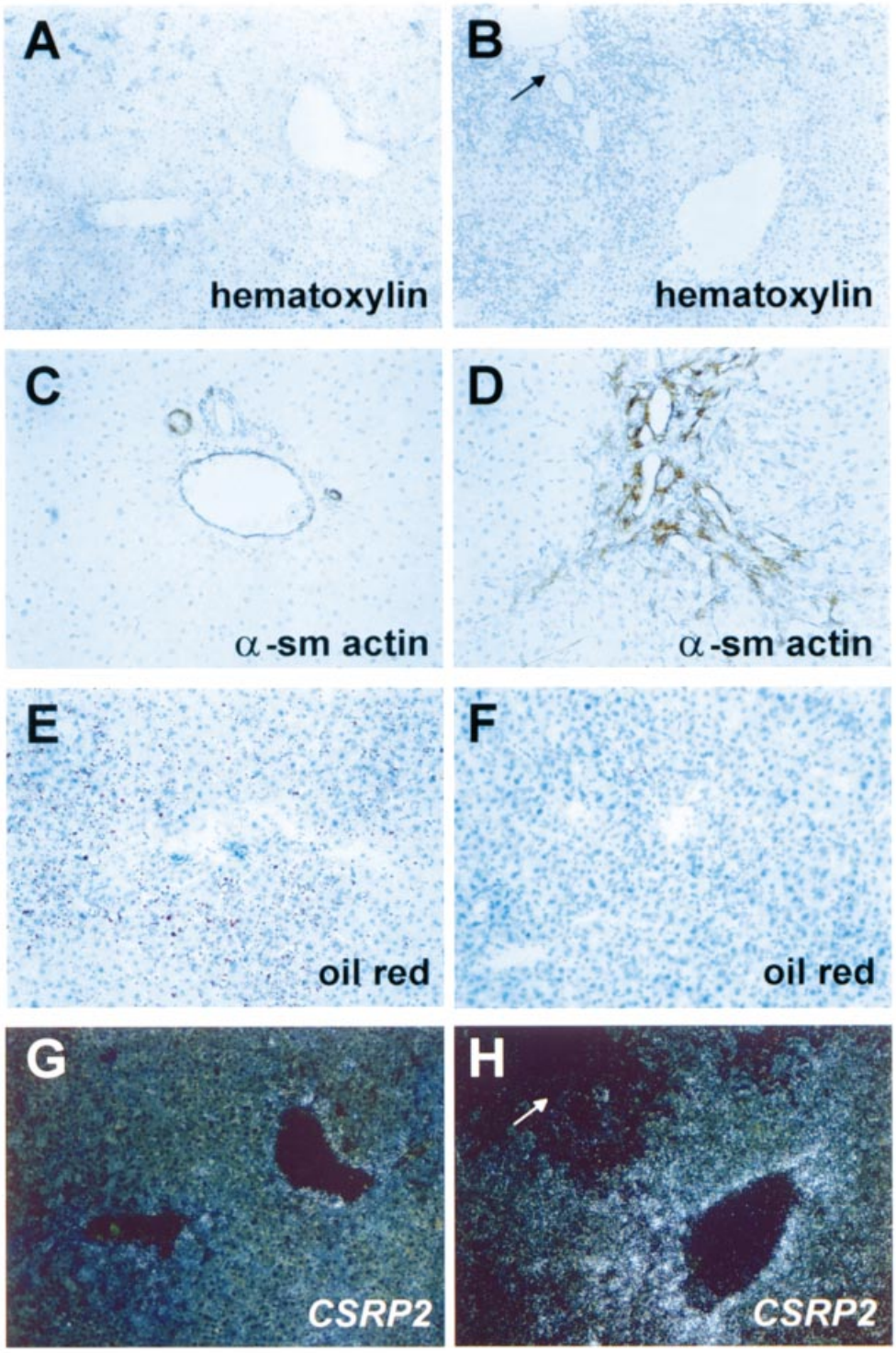

Figure 3 Expression *in vivo* of *CSRP2* in normal and cholestatic liver

(**A**, **B**) Mayer's hematoxylin staining of normal (**A**) and fibrotic (**B**) liver sections. (**C**, **D**) Detection of α-SMA (α-sm actin) by a three-step immunoperoxidase method in the portal zone of normal (**C**) and bile-duct-ligated (**D**) rat. The colour reaction was developed with the Vectastain-ABC kit and tissue sections were counterstained with Mayer's haematoxylin. In normal liver (**C**), α-SMA immunoreactivity is confined to the media of portal tract vessels, whereas in the liver from a rat whose bile duct has been ligated for 20 days (**D**) an increase in α-SMA-positive cells surrounding the proliferating bile ductules is observed. Some α-SMA-positive cells extend into the adjacent liver parenchyma. (**E**, **F**) Staining of normal (**E**) and fibrotic (**F**) liver sections with Oil Red O. In normal liver, intracellular lipid droplets containing vitamin A are effectively stained. (**G**, **H**) *In situ* hybridization analysis of sections from (**A**) and (**B**) reveal strong *CSRP2* expression in regions of maximal activation of HSCs. Regions of fully transdifferentiated MFBs show no expression of *CSRP2* (white arrow in H, black arrow in B). Magnification values: (**A**, **B**, **G** and **H**), ×50; (**C**–**F**), ×100.

© 2001 Biochemical Society

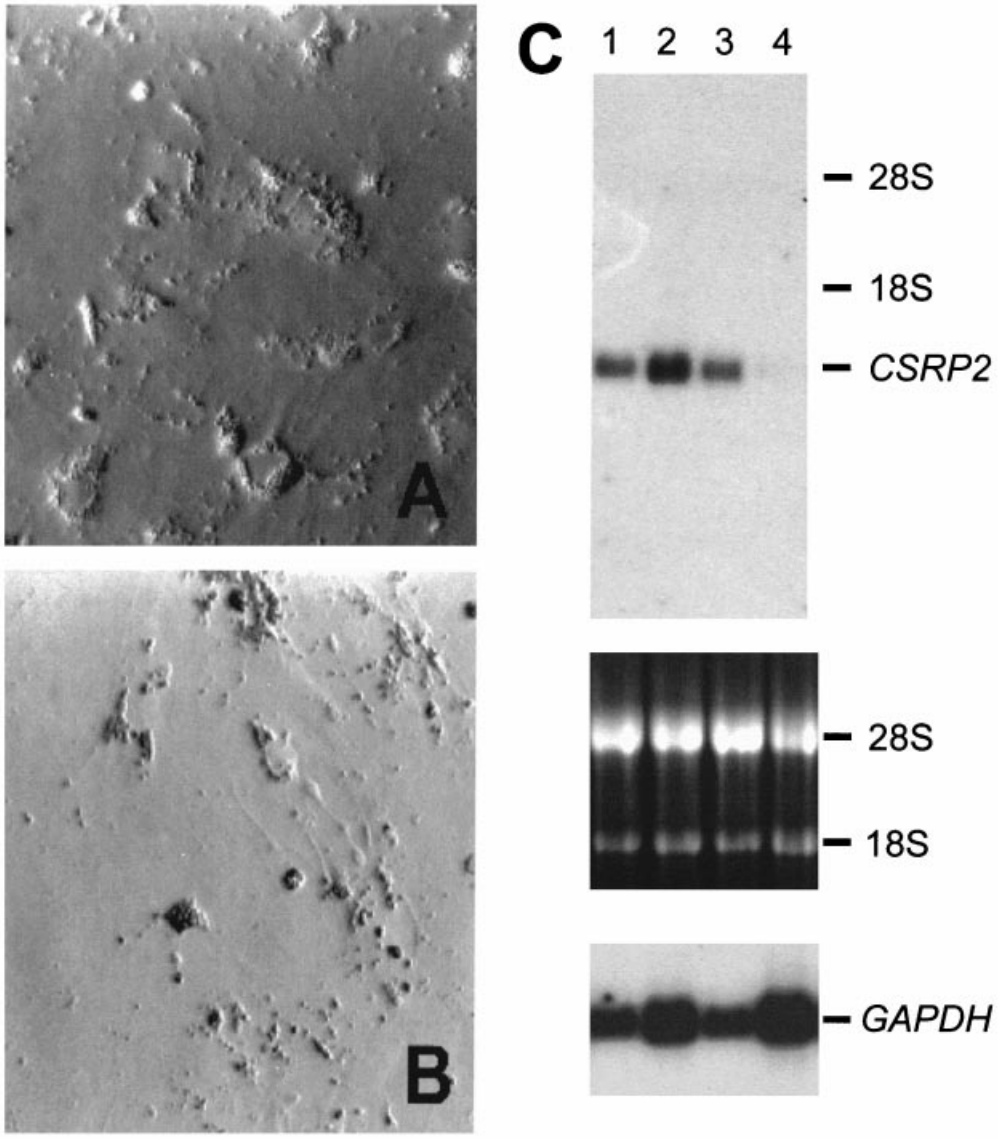

Figure 4 Activation of HSCs and expression of *CSRP2* is stimulated by PDGF-BB

(**A**) Nomarski microscopy of rat HSCs 4 days after primary culture, showing typical intracellular droplets of vitamin A. (**B**) Cells in parallel were treated with 40 ng/ml recombinant rat PDGF-BB, resulting in a myofibroblastic morphology (magn. $\times 320$). (**C**) A Northern-blot analysis of equal quantities (10 μg) of total cellular RNA from unstimulated (lane 1), PDGF-BB-stimulated (lane 2) or TGF-β_1-treated (lane 3) HSCs and from cell line CSFC-2G (lane 4) is shown. The blotted RNA species were hybridized with an [α-^{32}P]dCTP-labelled rat *CSRP2* cDNA. The intensities of 28 S and 18 S rRNA species were used as internal loading controls. The RNA species were rehybridized with a [α-^{32}P]dCTP-labelled GAPDH-specific cDNA probe.

activator domain. Elongation factor 1-α showed a low affinity for CRP2 and interaction was not analysed further. An artificial hydrophobic peptide and a phenylalanine-rich sequence isolated several times showed a strong interaction (group 3). These interactions might have been due to the overall hydrophobicity of those sequences and non-specific binding to hydrophobic patches within one or both LIM domains. However, two identified proteins were assigned to group 4 on the basis of their overall biochemical properties. Both proteins were able to interact with CRP2. We have recently described the identity of one of them [37]. The 1293 bp insert of the second interacting partner (prey clone 75) was sequenced. The cDNA-derived amino acid sequence was 353 residues in length. A GenBank® search with the BLAST algorithm at the NCBI (http://www.ncbi.nlm.nih.gov) revealed that the deduced amino acid sequence was identical to the C-terminus of PIAS1.

Determination of binding site

LIM domains of various proteins adopt a highly conserved tertiary structure. Both LIM domains (LIM1 and LIM 2) within CRP2 are independent folding units, separated by a flexible linker region [19] compatible with the proposed adapter function. If the interaction of CRP2 with PIAS1 is specific for CRP2 and not a general intrinsic property of the LIM domain itself, one would expect that PIAS1 would bind to one LIM domain of CRP2. To map the interacting interfaces and to determine the

© 2001 Biochemical Society

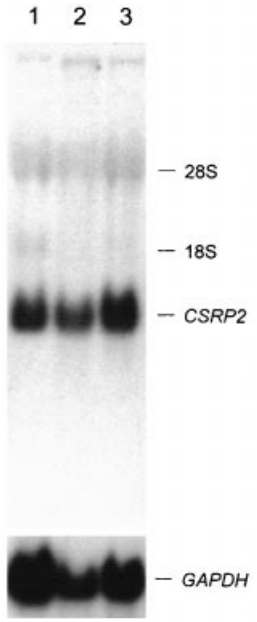

Figure 5 Expression of *CSRP2* in kidney and fibroblasts

A Northern-blot analysis with equal amounts (10 μg) of total cellular RNA from two biopsies of human tumorigenic kidney tissue (lanes 1 and 2) and the human fibroblast cell line WI-26 (lane 3) is shown. The blot was rehybridized with a GAPDH-specific cDNA probe.

contribution of the individual LIM domains of CRP2 to its interaction with PIAS1, deletion constructs were prepared (Figure 6A). As a further control, the quail CRP2 homologue (qCRP2), which was the first identified CRP2 [3], was used as a bait in these interaction studies. As depicted in Figure 6(B), positive growth and β-gal activity were detected in yeasts harbouring expression plasmids for quail CRP2, human CRP2 or the LIM2 domain of human CRP2 (encompassing residues 82–193). No reporter activity was monitored with the LIM1 domain of human CRP2 (encompassing residues 1–81). These results confirm the initial interaction of CRP2 and PIAS1 and reveal that LIM2 is necessary and sufficient for the interaction.

Co-localization and co-immunoprecipitation of CRP2 and PIAS1 in the cellular environment

Protein–protein interactions identified by the yeast two-hybrid assay need to be confirmed independently in the relevant biological system. To explore the CRP2–PIAS1 interaction in mammalian cells we transiently overexpressed full-length CRP2 and the Myc-tagged C-terminal part of PIAS1 in NIH-3T3 cells. The proper expression of both proteins was confirmed by Western blot analysis of cell extracts with an antibody specific for CRP2 or the Myc epitope (results not shown). Transiently expressed CRP2 alone displayed the typical subcellular localization with the reported actin-associated and nuclear distributions [5] (results not shown). The C-terminal part of PIAS1 containing a putative bipartite nuclear localization signal [$KK(X)_9KK$] (single-letter amino acid codes) at amino acid position 367–379 showed, when expressed in NIH-3T3 cells, essentially the same nuclear localization as that published previously for full-length PIAS1 [43] (results not shown). Untransfected controls showed only weak immunostaining with the CRP2-specific antiserum and no staining with the Myc-epitope-specific antibody (results not shown). Confocal laser scanning microscopy of cells transiently expressing both proteins revealed that CRP2 and PIAS1 were co-distributed along the cytoskeleton and within the cell nucleus (Figures 7A and 7B). The co-localization of both proteins is consistent with their interaction in cytosol and nucleus (Figure 7C). Independent verification of the interaction between CRP2 and PIAS1 was subsequently performed by co-immunoprecipitation assays. Cell lysates from the HEK-293 cell line transiently expressing CRP2 derivatives, a Myc-epitope-tagged PIAS1 or both were incubated with a CRP2-specific antisera, and co-precipitating PIAS1 was detected by Western blotting with a monoclonal antibody against the Myc epitope. As shown in Figure 7(D), PIAS1 specifically co-precipitated with CRP2 in this assay.

Chromosomal localization of the human PIAS1 gene locus

Although PIAS1 was assigned during the Human Genome Project to chromosome 15 (see accession number NT-010351), the exact chromosomal location of PIAS1 is unknown. We

Table 1 Identification of CRP2-interacting proteins/peptides by interaction trap

The identities of proteins were deduced by the sequencing of individual prey inserts; the reading frames of mitochondrial and cytosolic proteins vary from +1, +2 and +3 respectively.

Group	Protein/peptide	Accession number
1. Mitochondrial proteins	Human mitochondrion cytochrome *b*	HSU09500
	Human cytochrome *c* oxidase	NC_001807
	Human NADH dehydrogenase, subunit 4	NC_001807
	Human mitochondrial RNA	NC_001807
	Human 16 S rRNA	NC_001807
	Human kidney catalase	X04076
	Human WNT2B	NM_004185
2. Cytosolic proteins	Human elongation factor 1-α	X16869
	Human cyclophilin	X52851
	Human uracil DNA glycosylase/GAPDH	X53778
	Human uromodulin	NM_003361
3. Artifical hydrophobic peptides	... LMIYEFYY	
	... AAASTRASFFFFFFFF ...	
4. Specific interactors	Human PIAS	AF167160
	Human novel protein (CRP2BP)	HSJ717M23*

* The second interacting partner was recently published in detail elsewhere [37].

© 2001 Biochemical Society

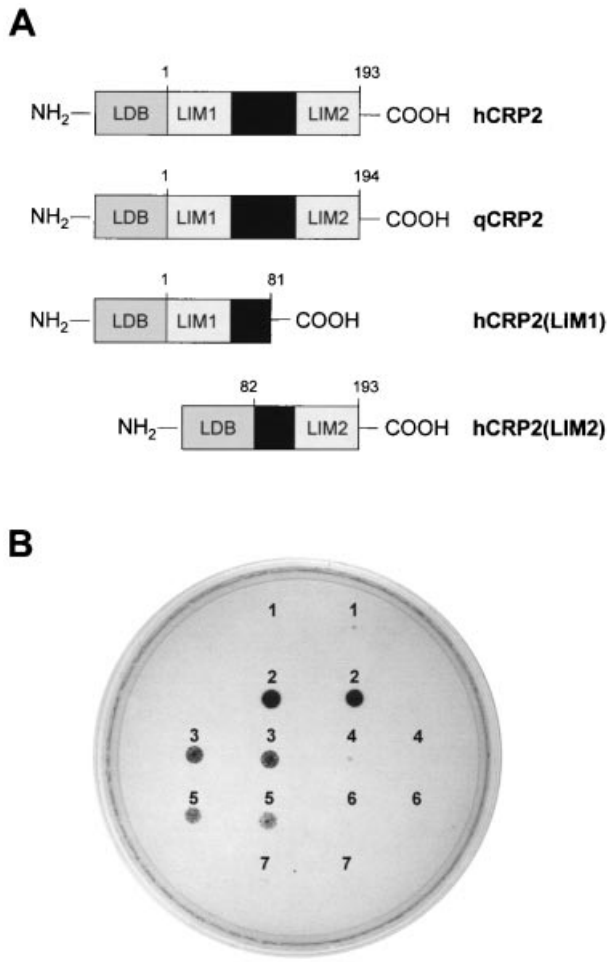

Figure 6 Interaction of PIAS1 with the LIM2 domain of CRP2

(**A**) Human full-length CRP2 (hCRP2), quail full-length CRP2 (qCRP2), the LIM1 domain of human CRP2 [hCRP2(LIM1)] and the LIM2 domain of human CRP2 [hCRP2(LIM2)] were fused to the LexA DNA-binding moiety (LDB). (**B**) PIAS1 (residues 298–650) was tested for binding activity with hCRP2, qCRP2, hCRP2(LIM1) or hCRP2(LIM2). Transformants were selected on SD/—Ura/—His/—Trp minimal selection plates and two individual colonies each were spotted on SD/Gal/Raf/—Ura/—His/—Trp/—Leu/X-Gal/BU-salts minimal plates. Selection for interaction was performed for 40 h at 30 °C. Transformants were pLexA and pB42AD (spot 1), pLexA(qCRP2) and pB42AD-no75 (spot 2), pLexA(hCRP2) and pB42AD-no75 (spot 3), pLexA[hCRP2(LIM1)] and pB42AD-no75 (spot 4), pLexA[hCRP2(LIM2)] and pB42AD-no75 (spot 5), pLexA(hCRP2) and pB42AD (spot 6) and pLexA and pB42AD-no75 (spot 7). Both yeast cell growth (Leu^+) and colour development (β-gal^+) were used as criteria for positive interaction.

therefore performed a precise mapping of PIAS1 by the FISH technique. As expected, specific fluorescent signals were obtained on chromosome 15 with a PIAS1-specific probe (Figure 8). In addition to direct visualization of the fluorescent profile signals on the DAPI/propidium iodide-banded chromosomes, we used the comparative genomic hybridization ('CGH') analysis software to determine the chromosomal locations of the hybridized probes. Both methods showed that the PIAS1 hybridization doublets were localized to chromosome sub-band 15q22.

DISCUSSION

CSRP2 was originally discovered on the basis of its strong suppression in avian fibroblasts transformed by retroviral oncogenes or chemical carcinogens [3]; the suppression of *CSRP2* and its gene product, CRP2, was later directly linked to the transformed phenotype of fibroblasts in conditional transformation systems [1,13].

In accordance with cellular transformation, quiescent HSCs undergo mitogenic activation during the process of transdifferentiation. Active proliferation, increased expression of extracellular matrix components, enhanced contractility and the secretion of fibrogenic mediators are the main characteristics of MFBs. This process has attracted considerable attention because it is the key event in the pathogenesis of liver fibrosis. We studied the expression of *CSRP2* in this process by using models both *in vitro* and *in vivo*. *CSRP2* expression in liver is restricted to HSCs and the activation of HSCs is accompanied by an initial moderate up-regulation of *CSRP2* and a suppression in later stages of transdifferentiation. Our Northern analysis further reveals that the initial increase in CSRP2 mRNA during transdifferentiation can be influenced by the administration of PDGF. In liver this cytokine is the most potent mitogenic stimulus for HSCs *in vivo* [44,45] and has marked effects on HSCs in culture. PDGF is also the major trigger for fibroblasts and smooth-muscle cells. It is noteworthy that *CSRP2* is expressed in all these PDGF-sensitive cells. These findings suggest that CRP2 function is linked to cytokine (PDGF) signalling pathways. In this context it is notable that overexpression of the closely related CRP3/MLP in myoblasts favours myogenic differentiation by decreasing their sensitivity to TGF-β_1 and that the expression of *CSRP1* encoding CRP1 is stimulated by serum factors [4,46].

The three-dimensional structure of CRP2 predicts a function as a molecular adapter protein [19]. To assign a distinct cellular function for CRP2 in the cytokine network we performed a yeast two-hybrid screen and found that PIAS1, a potent inhibitor of the JAK/STAT pathway, can interact with CRP2. This interaction of PIAS1 and CRP2 was demonstrated by three independent methods. First, we used CRP2-deletion constructs in the interaction trap to test the specificity of the observed interaction. The LIM2 domain of CRP2 is necessary and sufficient for binding to PIAS1, showing that the interaction is specific for that LIM domain and is not due to the general hydrophobic core structure present in LIM domains. Secondly, we performed co-localization experiments with recombinant proteins transiently expressed in mammalian cells. We demonstrate that CRP2 can bind to the last 353 residues of PIAS1 under cellular conditions, revealing that PIAS1 is a binding partner of CRP2 *in vivo*. Thirdly, the interaction between CRP2 and PIAS1 could be independently demonstrated by co-immunoprecipitation studies in the HEK-293 cell line. The closely related CRP3/MLP protein was shown previously to associate *in vivo* through the LIM1 domain with the muscle basic helix–loop–helix transcription factor MyoD in nucleus [6] and via the LIM2 domain with βI-spectrin in the cytosolic compartment [12]. Interestingly, in our experiments binding of CRP2 and PIAS1 is also observed in the nucleus and along the cytoskeleton in the cytosolic compartment.

PIAS1 is a pleiotropic protein effector with at least three distinct cellular functions. It was demonstrated that PIAS1 binds to the Gu/RNA helicase II [43], specifically inhibits STAT1-mediated gene activation [20] and functions as a nuclear receptor transcriptional co-regulator [47]. The adapter protein CRP2 might therefore interfere with the function of all these proteins by sequestering PIAS1 and masking relevant binding interfaces. Consistent with this hypothesis is the observation that PIAS1–STAT1 interaction is mediated through the CRP2-susceptible C-terminus of PIAS1 [48] (see Figure 6). It is conceivable that anchoring PIAS1 at the cytoskeleton or binding PIAS1 in the nucleus is associated with a suppression of PIAS1

© 2001 Biochemical Society

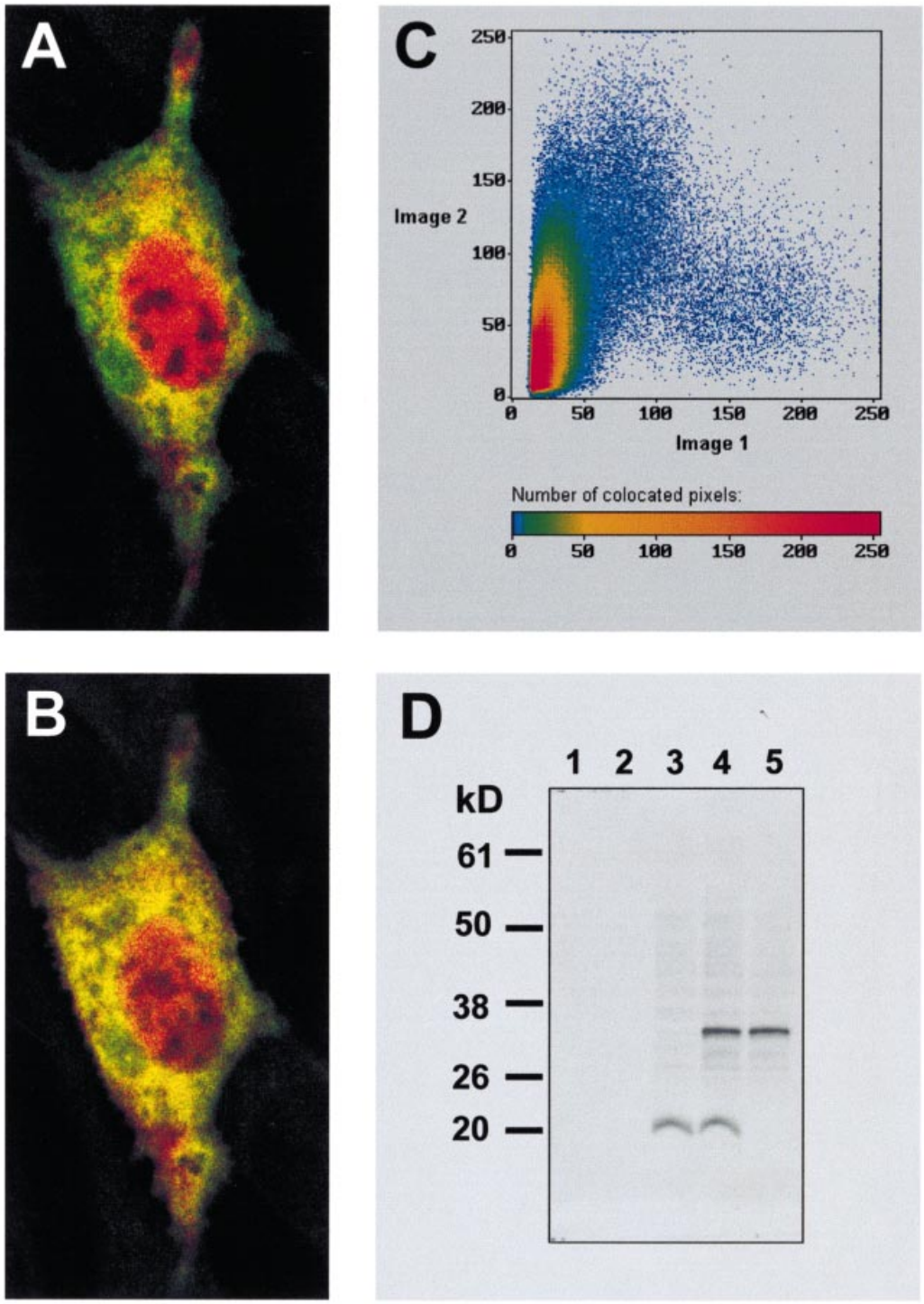

Figure 7 Interaction of CRP2 and PIAS1 in cellular environment

(**A** and **B**) (magnification $\times 1000$) c-Myc-epitope-tagged PIAS1 (residues 298–650) and human CRP2 were transiently transfected into NIH-3T3 fibroblasts. Double-labelling immunocytochemistry was used to determine the distribution of subcellular proteins. Antisera for the detection of PIAS1 were c-Myc monoclonal antibody (clone 9E10) and goat anti-mouse-IgG-Cy 3 (red channel). Antibodies for the detection of CRP2 were polyclonal antibody against CRP2, following biotinylated pig anti-rabbit antibody and FITC-conjugated streptavidin (green channel). Double-transfected NIH-3T3 cells were monitored for regional co-localization by confocal laser scanning microscopy along the *z*-axis. (**A** and **B**) are two images taken from different scans along the *z*-axis of one double transfected cell. Yellow areas are regions of common localization. No signals were observed with rabbit preimmune serum or non-specific murine IgG1 fraction performed in parallel (results not shown). (**C**) Distributions of CRP2 and PIAS1 along the *x*-axis and *y*-axis were overlaid. The numbers of co-located pixels ranged from 0 (no co-localization) to 250 (co-localization). (**D**) Co-immunoprecipitation of CRP2 and PIAS1 in HEK293 cells. Lysate proteins from mock-transfected HEK-293 cells (lane 1) and from HEK-293 cells transfected with Myc-PIAS (lane 2), Myc-CRP2 (lane 3), Myc-CRP2/Myc-PIAS1 (lane 4) or HA-CRP2/Myc-PIAS1 (lane 5) were immunoprecipitated with a CRP2-specific antiserum. The immunoprecipitates were subjected to SDS/PAGE, transferred on to a nitrocellulose membrane and probed with a monoclonal antibody against the Myc epitope. The positions of molecular mass markers are indicated (in kDa) on the left.

© 2001 Biochemical Society

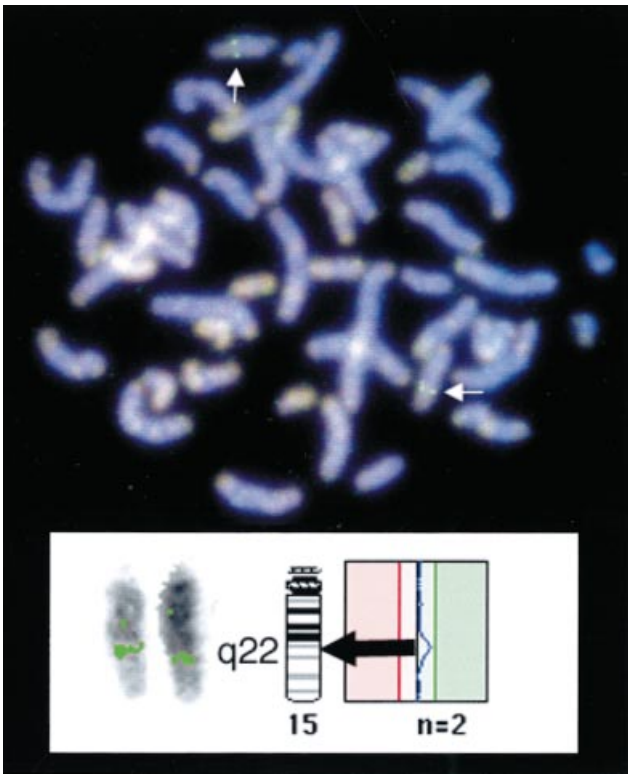

Figure 8 Chromosomal mapping of human PIAS1

Immunodetection of hybridized DNA from PIAS1 cDNA revealed with an FITC-specific filter combination on chromosomes counterstained with DAPI/propidium iodide. Fluorescent signals on the two homologous chromosomes are indicated by arrows. The inset shows a direct visualization of hybridization spots on DAPI-banded (blue channel) chromosomes (left) and the average ratio between green (FITC channel; biotinylated probe) and red (TRITC channel; propidium iodide counterstain) for two measured chromosomes compared with the respective ideogram (right). The assignment of the fluorescence peak to the corresponding sub-band is indicated by an arrow.

function and activation of the JAK/STAT pathway. It is of interest to note that CRP proteins have three possible types of cellular distribution (nuclear, F-actin-associated, or both nuclear and F-actin-associated) within one cell type [5], raising the hypothesis that the distribution of CRP2 and CRP2/PIAS1 complexes has an impact on CRP2 function. A lack of CRP2 as a result of oncogenic transformation or cytokine-induced cell activation leads to higher concentrations of active PIAS1 and therefore to altered amounts of free STAT factors, Gu/RH-II helicase or androgen receptors. Conceivable with that hypothesis is the observed overall altered gene expression during the pathogenesis of liver fibrosis and cellular transformation.

In addition, it has been demonstrated that PDGF directly activates JAKs and STATs [49,50]. It is possible that this activation is in part mediated by an altered expression of *CSRP2*. Indeed, we have shown recently that adenoviral overexpression of CRP2 is sufficient to potentiate the sensitivity of HSCs to PDGF (E. Van de Leur, A. M. Gressner and R. Weiskirchen, unpublished work).

Further studies are now required for an understanding of the fine-tuning of the JAK/STAT/PIAS/CRP2 network and its potential impact on oncogenic transformation and liver fibrosis.

We thank Mu-En Lee (Cardiovascular Biology Laboratory, Harvard School of Public Health, Boston, MA, U.S.A.) for kindly providing cDNA of rat CSRP2/SmLim, and Marcos Rojkind (Marion Bessin Liver Research Center, Albert Einstein College of Medicine, New York, NY, U.S.A.) for providing the cell line CFSC-2G. This work was supported by a grant from the Deutsche Forschungsgemeinschaft to R.W. (WE 2554\1).

REFERENCES

1 Weiskirchen, R., Pino, J. D., Macalma, T., Bister, K. and Beckerle, M. C. (1995) The cysteine-rich protein family of highly related LIM domain proteins. J. Biol. Chem. **270**, 28946–28954
2 Liebhaber, S. A., Emery, G., Urbanek, M., Wang, X. and Cooke, NE (1990) Characterization of a human cDNA encoding a widely expressed and highly conserved cysteine-rich protein with an unusual zinc-finger motif. Nucleic Acids Res. **18**, 3871–3879
3 Weiskirchen, R. and Bister, K. (1993) Suppression in transformed avian fibroblasts of a gene (*crp*) encoding a cysteine-rich protein containing LIM domains. Oncogene **8**, 2317–2324
4 Arber, S., Halder, G. and Caroni, P. (1994) Muscle LIM protein, a novel essential regulator of myogenesis, promotes myogenic differentiation. Cell **79**, 221–231
5 Arber, S. and Caroni, P. (1996) Specificity of single LIM motifs in targeting and LIM/LIM interactions *in situ*. Genes Dev. **10**, 289–300
6 Kong, Y., Flick, M. J., Kudla, A. J. and Konieczny, S. F. (1997) Muscle LIM protein promotes myogenesis by enhancing the activity of MyoD. Mol. Cell. Biol. **17**, 4750–4760
7 Louis, H. A., Pino, J. D., Schmeichel, K. L., Pomiès, P. and Beckerle, M. C. (1997) Comparison of three members of the cysteine-rich protein family reveals functional conservation and divergent patterns of gene expression. J. Biol. Chem. **272**, 27484–27491
8 Jain, M. K., Kashiki, S., Hsieh, C. M., Layne, M. D., Yet, S. F., Sibinga, N. E. S., Chin, M. T., Feinberg, M. W., Woo, I. and Maas, R. L. et al. (1998) Embryonic expression suggest an important role for CRP2/SmLIM in the developing cardiovascular system. Circul. Res. **83**, 980–985
9 Arber, S., Hunter, J. J., Ross, J., Hongo, M., Sansig, G., Borg, J., Perriard, J. C., Chien, K. R. and Caroni, P. (1997) MLP-deficient mice exhibit a disruption of cardiac cytoarchitectural organization, dilated cardiomyopathy, and heart failure. Cell **88**, 393–403
10 Pomiès, P., Louis, H. A. and Beckerle, M. C. (1997) CRP1, a LIM domain protein implicated in muscle differentiation, interacts with α-actinin. J. Cell Biol. **139**, 157–168
11 Schmeichel, K. L. and Beckerle, M. C. (1998) LIM domains of cysteine-rich protein 1 (CRP1) are essential for the zyxin-binding function. Biochem. J. **331**, 885–892
12 Flick, M. J. and Konieczny, S. F. (2000) The muscle regulatory and structural protein MLP is a cytoskeletal binding partner of βI-spectrin. J. Cell. Sci. **113**, 1553–1564
13 Oberst, C., Hartl, M., Weiskirchen, R. and Bister, K. (1999) Conditional cell transformation by doxycycline-controlled expression of the MC29 v-*myc* allele. Virology **253**, 193–207
14 Jain, M. K., Fujita, K. P., Hsieh, C. M., Endege, W. O., Sibinga, N. E. S., Yet, S. F., Kashiki, S., Lee, W. S., Perella, M. A., Haber, E. and Lee, M. E. (1996) Molecular cloning and characterization of SmLIM, a developmentally regulated LIM protein preferentially expressed in aortic smooth muscle cells. J. Biol. Chem. **271**, 10194–10199
15 Heldin, C. H. and Westermark, B. (1999) Mechanism of action and *in vivo* role of platelet-derived growth factor. Physiol. Rev. **70**, 1283–1316
16 Friedman, S. L. (2000) Molecular regulation of hepatic fibrosis, an integrated cellular response to tissue injury. J. Biol. Chem. **275**, 2247–2250
17 Gressner, A. M. (1996) Transdifferentiation of hepatic stellate cells (Ito cells) to myofibroblasts: a key event in hepatic fibrogenesis. Kidney Int. **49**, S39–S45
18 Pinzani, M., Marra, F. and Carloni, V. (1998) Signal transduction in hepatic stellate cells. Liver **18**, 2–13
19 Konrat, R., Kräutler, B., Weiskirchen, R. and Bister, K. (1998) Structure of cysteine- and glycine-rich protein CRP2: backbone dynamics reveal motional freedom and independent spatial orientation of the LIM domains. J. Biol. Chem. **273**, 23233–23240
20 Liu, B., Liao, J., Rao, X., Kushner, S. A., Chung, C. D., Chang, D. D. and Shuai, K. (1998) Inhibition of Stat1-mediated gene activation by PIAS1. Proc. Natl. Acad. Sci. U.S.A. **95**, 10626–10631
21 Seglen, P. O. (1976) Preparation of rat liver cells. Methods Cell. Biol. **13**, 29–83
22 De Leeuw, A. M., McCarthy, S. P., Geerts, A. and Knook, D. L. (1984) Purified rat liver fat-storing cells in culture divide and contain collagen. Hepatology **4**, 392–403
23 Schäfer, S., Zerbe, O. and Gressner, A. M. (1987) The synthesis of proteoglycans in fat-storing cells of rat liver. Hepatology **7**, 680–687
24 Knook, D. L., Blansjaar, N. and Sleyster, E. C. (1977) Isolation and characterization of Kupffer and endothelial cells from the rat liver. Exp. Cell. Res. **109**, 317–329

© 2001 Biochemical Society

25 Gressner, A. M., Lotfi, S., Gressner, G., Haltner, E. and Kropf, J. (1993) Synergism between hepatocytes and Kupffer cells in the activation of fat storing cells (perisinusoidal lipocytes). J. Hepatol. **19**, 117–132
26 Zerbe, O. and Gressner, A. M. (1988) Proliferation of fat-storing cells in stimulated by secretions of Kupffer cells from normal and injured liver. Exp. Mol. Pathol. **49**, 87–101
27 Kountouras, J., Billing, B. H. and Scheuer, P. J. (1984) Prolonged bile duct obstruction: a new experimental model for cirrhosis in the rat. Br. J. Exp. Pathol. **65**, 305–311
28 Weiskirchen, R., Erdel, M., Utermann, G. and Bister, K. (1997) Cloning, structural analysis, and chromosomal localization of the human *CSRP2* gene encoding the LIM domain protein CRP2. Genomics **44**, 83–93
29 Gyuris, J., Golemis, E., Chertkov, H. and Brent, R. (1993) Cdil, a human G1 and S-phase protein phosphatase that associates with Cdk2. Cell **75**, 791–803
30 Ito, H., Fukada, Y., Murata, K. and Kimura, A. (1983) Transformation of intact yeast cells treated with alkali cations. J. Bacteriol. **153**, 163–168
31 Schiestl, R. H. and Gietz, R. D. (1989) High efficiency transformation of intact cells using single stranded nucleic acids as a carrier. Curr. Genet. **16**, 339–346
32 Hill, J., Donald, K. A. and Griffiths, D. E. (1991) DMSO-enhance whole cell yeast transformation. Nucleic Acids Res. **19**, 5791
33 Gietz, D., Jean, S., Woods, R. A. and Schiestl, R. H. (1992) Improved method for high efficiency transformation of intact yeast cells. Nucleic Acids Res. **20**, 1425
34 Golemis, E. A., Serebriiski, I., Finley, R. L., Kolonin, M. G., Gyuris, J. and Brent, R. (2001) Interaction trap/two-hybrid system to identify interacting proteins. In Current Protocols in Molecular Biology (Ausubel, F. M., Brent, R., Kingston, R. E., Moore, D. D., Seidman, J. G., Smith, J. A., and Struhl, K., eds), unit 20.1, John Wiley & Sons, New York
35 Estojak, J., Brent, R. and Golemis, E. A. (1995) Correlation of two-hybrid affinity data with *in vitro* measurements. Mol. Cell. Biol. **15**, 5820–5829
36 Hoffman, C. S. (2001). Preparation of DNA, RNA, and protein extracts from yeast. In Current Protocols in Molecular Biology. (Ausubel, F. M., Brent, R., Kingston, R. E., Moore, D. D., Seidman, J. G., Smith, J. A. and Struhl, K., eds), unit 13.11–13.13, John Wiley & Sons, New York
37 Weiskirchen, R. and Gressner, A. M. (2000) The cysteine- and glycine-rich LIM domain protein CRP2 specifically interacts with a novel human protein (CRP2BP). Biochem. Biophys. Res. Commun. **274**, 655–663
38 Loo, D. T., Kanner, S. B. and Aruffo, A. (1998) Filamin binds to the cytoplasmic domain of the β_1-integrin. J. Biol. Chem. **273**, 23304–23312
39 Ranganna, K. and Yatsu, F. M. (1997) Inhibition of platelet-derived growth factor BB-induced expression of glyceraldehyde-3-phosphate dehydrogenase by sodium butyrate in rat vascular smooth muscle cells. Arterioscler. Thromb. Vasc. Biol. **17**, 3420–3427
40 Greenwel, P., Rubin, J., Schwartz, M., Hertzberg, E. L. and Rojkind, M. (1993) Liver fat-storing cell clones obtained from a CCl_4-cirrhotic rat are heterogeneous with regard to proliferation, expression of extracellular matrix components, interleukin-6, and connexin 43. Lab. Invest. **69**, 210–216
41 Sadler, I., Crawford, A. W., Michelsen, J. W. and Beckerle, M. C. (1992) Zyxin and cCRP: two interactive LIM domain proteins associated with the cytoskeleton. J. Cell Biol. **119**, 1573–1587
42 Brent, R. and Finley, R. L. (1997) Understanding gene and allele function with two-hybrid methods. Annu. Rev. Genet. **31**, 663–704
43 Valdez, B. C., Henning, D., Perlaky, L., Busch, R. K. and Busch, H. (1997) Cloning and characterization of Gu/RH-II binding protein. Biochem. Biophys. Res. Commun. **234**, 335–340
44 Pinzani, M., Gesualdo, L., Sabbah, G. M. and Abboud, H. E. (1989) Effects of platelet-derived growth factor and other polypeptide mitogens on DNA synthesis and growth of cultured rat liver fat-storing cells. J. Clin. Invest. **84**, 1786–1793
45 Pinzani, M., Knauss, T. C., Pierce, G. F., Hsieh, P., Kenney, W., Dubyak, G. R. and Abboud, H. E. (1991) Mitogenic signals for platelet-derived growth factor isoforms in liver fat-storing cells. Am. J. Physiol. **260**, C485–C491
46 Wang, X., Lee, G., Liebhaber, S. A. and Cooke, N. E. (1992) Human cysteine-rich protein: a member of the LIM/double-finger family displaying coordinate serum induction with c-*myc*. J. Biol. Chem. **267**, 9176–9184
47 Tan, J., Hall, S. H., Hamil, K. G., Grossman, G., Petrusz, P., Liao, J., Shuai, K. and French, F. S. (2000) Protein inhibitor of activated STAT-1 (signal transducer and activator of transcription-1) is a nuclear receptor coregulator expressed in human testis. Mol. Endocrinol. **14**, 14–26
48 Liao, J., Fu, Y. and Shuai, K. (2000) Distinct roles of the NH_2- and COOH-terminal domains of the protein inhibitor of activated signal transducer and activator of transcription (STAT) 1 (PIAS1) in cytokine-induced PIAS1–Stat1 interaction. Proc. Natl. Acad. Sci. U.S.A. **97**, 5267–5272
49 Leaman, D. W., Leung, S., Li, X. and Stark, G. R. (1996) Regulation of STAT-dependent pathways by growth factors and cytokines. FASEB J. **10**, 1578–1588
50 Vignais, M. L., Sadowski, H. B., Watling, D., Rogers, N. C. and Gilman, M. Z. (1996) Platelet-derived growth factor induces phosphorylation of multiple JAK family kinases and STAT proteins. Mol. Cell. Biol. **16**, 1759–1769

Received 26 June 2001/7 August 2001; accepted 24 August 2001

© 2001 Biochemical Society